ZEUGMA BIOLOGICAL SCIENCE

ZEUGMA
BIOLOGICAL SCIENCE

2025
v:5 n:2 p:16-41

Evaluation of Unripe *Musa paradisiaca* Pulp Extract in Streptozotocin-induced Type-2 Diabetic Rats: *In-vivo* Studies and *In-silico* Modelling

Olasunkanmi Kayode Awote[1]* and Ayomide Aleemat Abass[1]

[1] Department of Biochemistry, Lagos State University, PMB 001, Ojo, Lagos, Nigeria.

olasunkanmi.awote@lasu.edu.ng

Abstract:

Diabetes mellitus is still a major public health problem that comes with a lot of complications in both young and old individuals. *Musa paradisiaca* is abundant in the tropical and sub-tropical regions of Africa and has several medicinal traditional claims. Hence, this study evaluated the effect of *Musa paradisiaca* aqueous pulp extract (MPAPE) in STZ-induced diabetic rats. Bioactive compounds of MPAPE were identified and quantified using gas chromatography-mass spectroscopy (GC-MS) and high-performance liquid chromatography (HPLC) techniques. A total of 24 male Wistar rats were divided into 4 groups (n=6), including control, diabetic-untreated, and diabetic-treated groups (with MPAPE or glibenclamide). Oxidative stress (hydrogen peroxide [H_2O_2], nitric oxide [NO], malondialdehyde [MDA], glutathione [GSH]); lipid profile (total cholesterol [TC], triglyceride [TRIG], high-density [HDL-Chol, low-density [LDL-Chol], and very-low-density [VLDL-Chol] lipoprotein cholesterol; liver antioxidant (superoxide dismutase [SOD], catalase [CAT]); and liver function (alanine [ALT], and aspartate [AST] aminotransferase) enzymes were evaluated using standard biochemical kits and procedures. PyRx and Biovia Discovery Studio were used for molecular docking studies, while SwissADME and ProTox were used to predict the ADME/T properties. The results of the phytochemistry of *M. paradisiaca* pulp showed the presence of alkaloids, tannins, flavonoids, saponins, and phenols, with an abundant polyphenolic content. The administration of MPAPE (300 mg/kg body weight) significantly ($p<0.05$) decreased the high levels of glucose, total-chol, LDL-chol, TRIG, VLDL-chol, H_2O_2, NO, MDA, and the activities of SOD and CAT while, decreasing ALT and AST activities, and HDL- Chol, and GSH levels. In conclusion, MPAPE may possess antioxidant and antidiabetic potentials in the management of diabetes.

Keywords: Traditional medicine, Medicinal plants, Nutraceuticals, *Musa paradisiaca* fruit, Oxidative stress, Diabetes, Liver damage, Antioxidant, Streptozotocin, Phytochemistry.

Introduction

Oxidative stress, an imbalance between oxidants and antioxidants, leads to a disruption in redox signaling and regulation (Azzi, 2022). This results in the overproduction and accumulation of reactive oxygen species (ROS), which play a role in the development of a myriad of maladies, including diabetes, cardiovascular diseases, cancers, neurodegenerative diseases, aging, and respiratory diseases. The source of production of ROS can either be environmental stressors (e.g., ultraviolet light, heavy metals, ionizing radiation, and smoke) or within an individual (i.e, mitochondrial dysfunction, lipoxygenase, cyclooxygenase, and peroxisomes) (Singh *et al*., 2022). Several antioxidants, which can either be synthesized by the cells or obtained daily from diets, have been utilized in recent times to stabilize or deactivate free radicals (Marino *et al*., 2022).

Streptozotocin (STZ), isolated from *Streptomyces achromogenes*, is the most common diabetogenic chemical extensively used in experimental animals for creating animal models of Type 1 and Type 2 diabetes. Proper preparation and administration of STZ are essential for obtaining reliable results from the animal models of diabetes produced by the drugs (Furman, 2015; Ghasemi and Jeddi, 2023).

Diabetes mellitus (DM) is a modern pandemic and consistently high blood sugar (hyperglycemia) metabolic disease caused by a malfunction in either the action or secretion of insulin, or both. Chronic high blood sugar (hyperglycemia) caused by insulin deficiency usually disrupts the metabolism of proteins, fats, and carbohydrates. Tissue or vascular damage develops as the condition worsens, resulting in serious diabetic complications like neuropathy, retinopathy, and cardiovascular problems (Onah and Oguche, 2022). Long-term damages, such as macrovascular and microvascular damage, can both be attributed to the persistent hyperglycemic state that causes the majority of problems associated with DM. Currently, well-recognized macrovascular implications include the increasing prevalence of myocardial infarctions and brain injuries as a result of arteriosclerotic abnormalities of the large-diameter arteries, which induce a progressive reduction in the diameter of the vessels. Microvascular problems, on the other hand, impact the small-diameter vessels and peripheral circulation, affecting the central and peripheral nerve systems, lower limbs, kidneys, and eyes (Ortiz *et al*., 2022). In 2019, 436 million adults worldwide were estimated by the International Diabetes Federation (IDF) to have diabetes, and the number is predicted to nearly double by 2030 (Seedi *et al*., 2019; Adeniran *et al*., 2022). Among the countries in sub-Saharan Africa, Nigeria is currently experiencing an increase in the prevalence of diabetes mellitus, with approximately 3.7% of adult Nigerians (20-79 years) living with DM according to a recent IDF report (Fasula *et al*., 2024).

Conventional antidiabetic drugs such as sulfonylureas, biguanides, α-glucosidase inhibitors, agonists for peroxisome proliferator-activated receptor-γ (PPARγ), inhibitors of dipeptidyl peptidase IV (DPP IV), and inhibitors of sodium-glucose co-transporter-2 (SGLT2) are economical and the prolonged use of these medications has been associated with serious side effects including the risk of coma, edema, hypoglycemia, vomiting, bloating, possible weight gain, and issues with the central nervous and cardiovascular systems (Banu and Bhowmick, 2017, Daliri *et al*., 2017; Padhi *et al*., 2020). Therefore, to alleviate these side effects, new therapeutic approaches are required, and natural products have been reported as safe and natural alternatives (Yedjou *et al*., 2023), including medicinal plants.

Medicinal plants do not only serve as a food source but also for their therapeutic effects, including antioxidant defenses, cell proliferation, expression of genes, and maintenance of mitochondrial integrity (Adetuyi *et al*., 2022). Herbal remedies have been used to treat diseases worldwide since the beginning of time; thus, much attention has been given to natural products influencing the development of new drugs. The plant diversity in West Africa, including Nigeria, is very abundant, and African traditional medicine is one of the most ancient medical systems in the world with its attributed low cost, safe history, and suitability in treating various diseases (Ayeni *et al*., 2022). *Musa paradisiaca* is a member of the family *Musaceae* (Fig. 1). Its species are widely spread in southern Asia, and tropical and subtropical regions of Africa (Kemisetti and Rajeswar Das, 2022). Many parts of this plant serve medicinal purposes, and it has been found to possess antidepressant, antihypertensive, antibacterial, antifungal, anti-ulcer, antioxidant, and anti-diabetic activity (Shree and Selvakumar, 2022). Despite the numerous biological activities attributed to this plant, there is limited information on the antioxidant and antidiabetic effects of MPAPE administration on streptozotocin-induced diabetic rats. Hence, this study is carried out using experimental and computational guided methodologies.

Figure 1: Pictorial view of *Musa paradisiaca* leaf and fruit (Google Search Engine, 2025).

Materials and Methods

Plant Collection and Extraction

Unripe fruits of *Musa paradisiaca* were purchased from a local market, Iyana-Iba market, Ojo, Lagos State, South-western Nigeria (6.4609° N, 3.2053° E), rinsed, cut into smaller sizes using a sterile knife, and left to air dry for 24 hours before homogenizing using a mortar and pestle. The resulting homogenate was weighed using an analytical balance, and 67.70 grams was added to a volumetric flask with 670 mL of deionized water in the ratio 1:10, where it was macerated for 48 hours. The resulting solution was filtered using a Whatmann grade 1 filter paper, heated for 30 minutes in a water bath at 40°C, and then stored in the refrigerator until needed.

Phytochemical Screening

The phytochemical components of MPAPE were determined using the methods described by Awote *et al*. (2024).

Gas Chromatography-Mass Spectroscopy (GC-MS) Analysis of *M. paradisiaca* Pulp Extract

An Agilent 5977B GC/MSD system with an Agilent 8860 auto-sampler, a gas chromatograph interfaced to a mass spectrometer (GC-MS) equipped with an Elite-5MS (5% diphenyl/95% dimethyl polysiloxane) fused a capillary column (30 × 0.25µm ID × 0.25µm df) were used to perform the GC-MS analysis of the extract. An electron ionization device with an ionization energy of 70 eV was used in electron impact mode for GC-MS detection. A split ratio of 10:1 was used with an injection volume of 1µL and helium gas (99.999%) as the carrier gas at a steady flow rate of 1 mL/min. To calibrate the GC-MS, five (5) point serial dilution calibration standards (1.25, 2.5, 5.0, and 10.0 ppm) were made from the 40 PPM stock solution. Temperatures were maintained at 300 °C for the injector, 250 °C for the ion source, and 100 °C (isothermal) for 0.5 min in the oven, with a 20 °C/min increase to 280 °C (2.5 min) for the oven. Mass spectra were obtained at 70 eV with a 0.5 s scanning interval and fragments ranging from

45 to 450 Da. GC/MS ran for a total of 21.33 minutes, with a solvent delay of 0 to 3 minutes (Awote *et al*., 2024).

High-Performance Liquid Chromatography (HPLC) Analysis of *M. paradisiaca* Pulp Extract.

The measurement of flavonoid components in the extracts was carried out using high-performance liquid chromatography (HPLC) on an HPLC-Agilent Technologies 1200 series liquid chromatograph equipped with a UV detector. A Hypersil BDS C18 column (150 × 4.6 mm, 5 µm particle size) prepacked for the reversed-phase was used for the chromatography, which was carried out at 250°C. A (0.1% formic acid in water) and B (HPLC grade acetonitrile) are combined to generate the mobile phase, which has a steady flow rate of 0.75 mL/min. At 0 min, 94% A, 14 min, 83.5% A, 16 min, 83% A, 18 min, 82.5% A, 20 min, 82.5%; 22–24 min, 81.5%; and 27–40 min, 80% A, the linear gradient solvent system began. The detection wavelength was 280 nm (Awote *et al*., 2021a).

***In-silico* Studies: Ligand Modeling**

The GC-MS and HPLC-generated ligands' 3D crystal structures were downloaded in .sdf format from the PubChem database (https://pubchem.ncbi.nlm.nih.gov/). Also, the ligands' canonical SMILES were downloaded from the PubChem database. Biovia Discovery Studios 2021 was used to convert the ligands to .pdb format, and Open Babel (https://openbabel.readthedocs.io/en/latest/Forcefields/mmff94.html) was utilized in optimizing the energy of the ligand molecules. Following energy minimization, the ligand molecules were converted specifically into pdbqt AutoDock ligand format (Awote *et al*., 2024).

Protein (Target) Preparation

The selected protein targets were sourced from the Protein Data Bank (https://www.rcsb.org) and a deposited crystal structure of Homo sapiens was used as a reference to model the 3D structures of these proteins. The protein grid box coordinates were set at x= 8.689, y= -27.9742, and z= 15.7172; x= -12.1777, y= -35.4768, and z= 88.7572; x= 80.183, y= 62.3450, and z= 3.4609; and

x= -0.3408, y= -0.6404, and z= 15. 0471 for human pancreatic α-amylase (PDB ID: 2QMK), human pancreatic α-glucosidase (PDB ID: 5NN8), human pancreatic sorbitol dehydrogenase (PDB ID: 1PL6), and aldose reductase (PDB ID: 3S3G), respectively, to target the active sites of each protein. Biovia Discovery Studio 2021 was used to eliminate heteroatoms, ligand groups, and water molecules from the protein structures and add hydrogen polar to protein structures to prepare them for molecular docking analysis (Awote *et al*., 2024).

Molecular Docking Profiling

The AutoDock Vina tool was utilized for molecular docking studies. The usual diabetes standard drugs, acarbose and tolrestat, and the co-crystallized ligands for the target proteins were utilized. Following the sorting of the ligand molecules according to increasing binding energies, the investigation was based on binding free energy values (Awote *et al*., 2024).

Absorption, Distribution, Metabolism, Excretion & Toxicity (ADMET) Properties Prediction

The top ten ligands were selected based on binding energy, and their drug-likeness parameters,

physicochemical properties, pharmacokinetic properties, lipophilicity, water solubility, medicinal chemistry, and toxicity were predicted using SwissADME and admetSAR. These predictive algorithms were used to evaluate the ligands' general eligibility as possible drug candidates and to offer information about their possible safety, pharmacological characteristics, and therapeutic efficacy (Awote *et al*., 2024).

Experimental Animals

Twenty-four (24) male Wistar rats (8 weeks old), with an average weight of 103 g (range of 100– 105 g), were sourced from the animal house of the Department of Biochemistry, Faculty of Science, Lagos State University, Nigeria. The rats were kept in regular day/night cycles while they were made to have access to clean drinking water and commercial pelleted feed (Vital feed® Nigeria). The current national and international criteria were followed in the care and usage of the Wistar rats during the study. With the ethical approval number LASU/23/REC/055, the Lagos State University Research Ethics Committee authorized the study procedure.

Induction of Type-2 Diabetes mellitus

Type-2 Diabetes Mellitus (T2DM) was introduced into the overnight fasted rats intraperitoneally at a dose of 60 mg/kg body weight of Streptozotocin (STZ) (Sigma-Aldrich Chemicals Company, St. Louis, MO., U.S.A.) dissolved in freshly prepared 0.1 M of iced-cold citrate buffer (pH 4.5) (Ogunyinka *et al*., 2017). To prevent hypoglycemia, the rats were maintained with 20% glucose (Unique Pharmaceuticals, Sango Otta, Ogun State, Nigeria) for six hours following the induction and later with 5% glucose for the following 24 hours. On the third day (72 hours) after induction, hyperglycemia was found to be gradually developing, but by the seventh day, all of the rats had stabilized and were consistently hyperglycemic. The rats exhibiting a fasting blood glucose level of 200 mg/dL or higher by the seventh day were classified as diabetic and included in the investigation. The fourth day after STZ induction marked the start of the treatments, which lasted for 28 days. The blood glucose concentrations were measured after drawing blood from the rats' tails using an Accu-Check glucometer. The success rate of induction exceeded 84.7%.

Animal Groupings and Treatments

Animal groupings and treatment were carried out using the modified method of Ogunyinka *et al*. (2017). Before this study, the rats were fasted overnight and divided into four (4) groups (A–D) of six rats each, randomly selected so that the group mean weights were the same.

Group A (normal control) consisted of non-diabetic rats that received 2 mL/kg body weight/day of distilled water orally for 28 days.

Group B (positive control) = streptozotocin (STZ)-induced diabetic rats orally administered 2 mL/kg body weight/ day distilled water for 28 days.

Group C = diabetic rats orally administered 300 mg/kg body weight/ day of *M. paradisiaca* pulp extract for 28 days.

Group D = diabetic rats orally administered 5 mg/kg body weight/ day of glibenclamide (®Daonil, Hoechst Marion Roussel Limited, Mumbai, India) for 28 days.

Blood Collection

After receiving medication for 28 days, each rat was given an injection of 0.1 mL of ketamine to induce anesthesia and then dissected. The gradual lack of corneal and pedal responses confirmed anesthesia. Afterward, a sterile 21G needle was placed on a 5 mL plunger syringe (Cliniject Hypodermic Syringe, Albert David Limited, Mandideep-462046, Raisen District, India) to collect fresh blood from the heart chamber, which was then stored in plain sample bottles. The blood was centrifuged immediately for 15 minutes at 2500 rpm. The supernatant (serum) was then removed and stored in the refrigerator until required for biochemical analysis.

Biochemical Assays

The effects of MAPAPE on STZ-induced diabetic Wistar rats were evaluated using the following biochemical parameters:

Protein Determination

The protein concentration of the various samples was determined using the Lowry method as described by Lowry *et al.* (1951) with a few modifications. In summary, 400 µL of solution C (200 µL solution B (1% copper sulfate ($CuSO_4.5H_2O$) and 2% sodium potassium tartrate) and 9.8 mL of solution A (0.1 M sodium hydroxide and 2% sodium bicarbonate), 40 µL of folin C, and 25 µL of each sample were mixed with 0.5 mg/mL bovine serum albumin (BSA). After thoroughly mixing, the mixture was left to stand. At 650 nm, the absorbance was measured against a blank that contained 60 µL of solution C, water, or buffer. From the Lowry standard curve, the protein concentrations of each group were extrapolated and expressed in mg/mL.

Catalase (CAT) Activity

Catalase activity was determined according to the method of Oladimeji *et al*. (2022). In summary, 10 µL of the homogenate and 590 µL of hydrogen peroxide (590 µL of 19 mM solution) were pipetted into a 1 cm quartz cuvette. The mixture was quickly swirled to mix it thoroughly, and it was then put in a spectrophotometer. The change in absorbance was measured at 240 nm for 10 seconds for 2 minutes. The extinction coefficient of hydrogen peroxide, which is 240 nm, was used to express catalase activity as µmol/mg protein.

Superoxide Dismutase (SOD) Activity

SOD activity was determined by the Epinephrine method reported by Oladimeji *et al*. (2023). In brief, 2.5 mL of 0.05 M phosphate buffer (pH 7.8) was mixed with 0.1 mL of the tissue homogenate supernatant. At the point of absorbance measurement, which was measured at 750 nm for one minute and thirty seconds at intervals of 15 seconds, 0.3 mL of adrenaline solution (0.059%) was then added. After calculation, SOD activity was then expressed as mmol/mg protein.

Lipid Profile Estimation

Using standard diagnostic test kits (Randox Laboratories, Crumlin, U.K.), the lipid profile (triglyceride (TG), total cholesterol (TC), and high-density lipoprotein cholesterol (HDL-c)) of the treated Wistar rats was analyzed in the liver homogenate and plasma sample. The Friedewald formula was used to determine plasma low-density lipoprotein cholesterol (LDL-c) and very-low-density lipoprotein cholesterol (VLDL-c): LDL-c = [TC- (HDL-c + TG/5)], and VLDL-c = TAG/5, respectively (Awote *et al*., 2021b).

Non-Protein Thiol (GSH) Estimation

The level of reduced glutathione (GSH) was estimated according to Jollow *et al*. (1974). Using Ellman's reagent (DTNB), the glutathione (GSH) content was determined calorimetrically. Sulfa-salicylic (4%) was added to the supernatant in a 1:1 ratio to precipitate it. After being stored at 4°C for one hour, the samples were centrifuged for ten minutes at 4°C at 5000 rpm. Phosphate buffer (0.1 M, 550 µL), 100 µL of supernatant, and 100 µL of DTNB were mixed to make up the assay combination. The absorbance was read at 412 nm, and the results were expressed as µmol of GSH/mg protein.

Nitric Oxide (NO) Estimation

After the Griess reaction, the concentrations of nitrite in serum or supernatants were determined by incubating 250 µL of the homogenate with 250 µL of Griess reagent at room temperature for 20 minutes. The spectrophotometric method was used to measure the absorbance at 550 nm. The absorbance of a standard solution containing known amounts of sodium nitrite was compared to determine the nitrite content; the findings were expressed as mmol/L (Green *et al*., 1983).

Hydrogen Peroxide (H_2O_2) Estimation

The FOX (ferrous oxidation-xylenol orange) assay was used to measure the levels of hydrogen peroxide. In brief, FOX is formed by adding 10 mL of Xylenol, 10 mL of sorbitol, and 50 mL of ammonium ferrous sulfate to 30 mL of distilled water. In the meantime, 10 µL of homogenate and 290 µL of FOX were well mixed by vortexing until foamy. After 30 minutes of room temperature incubation, a faint pink color complex is produced. At a wavelength of 560 nm, the absorbance was measured against a blank (distilled water). The hydrogen peroxide generated was calculated and expressed in mmol/mL (Wolff, 1994).

Lipid Peroxidation Estimation

Lipid peroxidation was determined by measuring the formation of thiobarbituric acid reactive substance (TBARS) according to the method of Varshney and Kale (1990). Briefly, tissue samples were homogenized in 0.1 M phosphate buffer (pH 7.4) in a ratio of 1:5. 200 µL of the stock reagent—an equal volume of trichloroacetic acid (10%, w/v) and 2-thiobarbituric acid (0.75%, w/v) in 0.1 M HCl was added to 100 µL of homogenate, and the mixture was incubated at 95ºC for an hour using a water bath. After cooling, the solution was centrifuged at 3000 rpm for 10 minutes, and the absorbance of the supernatant was measured at 532 nm and 600 nm. Lipid peroxidation was expressed as nmol.

Determination of Enzymatic Activities

Using commercial diagnostic kits (Randox, U.K.), the activities of alanine transaminase (ALT, EC 2.6.1.2) and aspartate transaminase (AST, EC 2.6.1.1) were measured following the manufacturer's instructions (Fagbohun *et al*., 2020). At 340 nm, each enzyme's activity was determined using a spectrophotometer.

Statistical Analysis

The results are presented as Mean ± Standard Error of Mean (SEM). For the descriptive statistics, One-way ANOVA was used to compare the treated and control groups using GraphPad Prism 5.0 (GraphPad Prism Software Inc., San Diego, CA, USA). When comparing

the treated and control groups, statistically significant differences were identified at $p<0.05$ with a 95% confidence interval. When significant, means were separated using the Bonferroni post-hoc test.

Results

The preliminary qualitative and quantitative (polyphenol content) of the aqueous pulp extract of *Musa paradisiaca* is presented in Table 1.1. Alkaloids, flavonoids, phenols, tannins, and saponins are all present. More so, the polyphenolic constituent screening of the extract showed an abundance of flavonoids, followed by phenols and tannins. The bioactive compounds found in MPAPE, as revealed by HPLC analysis, are presented in Table 1.2, with syringin (7.933 ppm) having the highest concentration, followed by kaempferol (6.333 ppm), quercetin (5.516 ppm), and luteolin (5.200 ppm). The bioactive compounds found in MPAPE, as revealed by GC-MS analysis, are presented in Table 1.3. The analysis showed the presence of 13 secondary metabolites with a total of 90.55 area percentages.

Table 1.1: Preliminary Phytochemical screening of *Musa paradisiaca* aqueous pulp extract

S. No.	Phytochemicals	Qualitative	Quantitative (mg/100g)
1	Alkaloids	+	NQ
2	Flavonoids	+	0.945 ± 0.78
3	Saponins	+	NQ
4	Phenols	+	0.641 ± 0.10
5	Steroids	-	NQ
6	Terpenoids	-	NQ
7	Tannins	+	0.182 ± 0.00

KEY: + = Present, - = Absent; NQ: not quantified

Table 1.2: Bioactive compounds of *Musa paradisiaca* aqueous pulp extract (MPAPE) analyzed with HPLC

S.No	Phytocompounds	Concentration (ppm)	Retention time (min)
1	Capsaicin	1.016	7.665
2	Caffeic acid	1.400	2.430
3	Beta-sistosterol	3.483	35.596
4	Apigenin	3.816	19.575
5	Luteolin	5.200	2.293
6	Quercetin	5.516	13.480
7	Kaempferol	6.333	36.260
8	Syringin	7.933	16.546

Table 1.3: Bioactive compounds of *Musa paradisiaca* aqueous pulp extract (MPAPE) analyzed with GC-MS

S.No	Phytocompounds	Molecular Weight*	Molecular Formula	Retention Time	Area (%)
1	1-Methylene-2b Hydroxymethyl-3,3-Dimethyl-4b-(3-Methylbut-2-Enyl)-Cyclohexane	222	$C_{15}H_{26}O$	33.776	5.59
2	3-Decyn-2-ol	154	$C_{10}H_{18}O$	21.296	10.9

3	26-Hydroxy Cholesterol	402	$C_{27}H_{46}O_2$	32.626	6.25
4	Campesterol	400	$C_{28}H_{48}O$	24.40	12.51
5	1,2-Benzenedicarboxylic acid, dioctyl ester (CAS) phthalate	390	$C_{24}H_{38}O_4$	25.768	10.18
6	Acetic Acid, 1-Methylethyl Ester	102	$C_5H_{10}O_2$	2.799	4.31
7	Methyl elaidate	296	$C_{19}H_{36}O_2$	20.605	2.16
8	Octadeca-9,12-Dienoic acid methyl ester	294	$C_{19}H_{34}O_2$	21.253	6.45
9	Hexadecanoic acid, methyl ester (CAS) Methyl palmitate	270	$C_{17}H_{34}O_2$	18.070	2.60
10	Octadecanoic acid, methyl ester (CAS) Methyl stearate	298	$C_{19}H_{38}O_2$	20.892	1.93
11	9-Octadecenamide, (Z)-	281	$C_{18}H_{35}NO$	23.51	15.97
12	Hexadecanoic acid (CAS) Palmitic acid	256	$C_{16}H_{32}O_2$	18.844	4.27
13	β-Stigmasterol	412	$C_{29}H_{48}O$	26.04	7.43

*Molecular weight in g/mol

The complex interaction of quercetin, the ligand with the best binding affinity, and the human pancreatic α-amylase protein is presented in Figure 2.1. The 2D structure illustrated the formation of a Pi-Pi T-shaped bond between the ligand and His201 (amino acids) at the surface of the protein. Additionally, Leu162 formed Pi-sigma and Pi-alkyl interactions with quercetin. Meanwhile, Trp59 forms a conventional hydrogen bond, and Leu165 forms a pi-alkyl interaction with quercetin. Additionally, Try151, Ile235, Glu233, Ala198, Asp197, His101, Glu60, Tyr62, and Gln63 all formed van der Waals interactions with quercetin. Figure 2.2 shows the 2D structure of campesterol – human α-glucosidase (protein) complex interaction. Ala555, Phe525, Trp481, Phe649, and Trp376 formed pi-alkyl and alkyl interactions with campesterol. Meanwhile, Leu650, Asp616, Asn524, Asp404, Asp282, Arg281, Ser253, Met519, Asp518, Arg600, His647, and Trp516 formed van der Waals interaction with the best binding affinity.

The 2D structure of the complex interaction between quercetin (ligand) and the human sorbitol dehydrogenase (protein) is presented in Figure 2.3. Ala254 forms an amide-pi stacked interaction, while Thr250, Leu204, and Ile233 form Pi-sigma and Ala252, Ala258, and Ile231 form Pi-alkyl bonds with quercetin. Additionally, Ser255, Cys178, Pro228, Ser227, and Gly179 formed van der Waals interactions with quercetin, while Thr202 and Glu226 formed a conventional hydrogen bond. Figure 2.4 illustrates the complex interaction between apigenin, the ligand with the best binding affinity, and the human aldose reductase protein. The 2D structure below illustrates the formation of a pi-alkyl bond between the ligand and Pro211 at the surface of the protein. Cys298 formed a pi-sulfur and conventional hydrogen bond with apigenin. Additionally, Trp20 and Tyr209 formed pi-pi stacked and pi-pi T-shaped bonds with apigenin, while Cys298, Ser210, and Asp43 formed a conventional hydrogen bond. More so, Pro215, Gly18, and Lys262 formed carbon-hydrogen bonds and pi-donor hydrogen bonds with the ligand apigenin. Meanwhile, Lys21, Asp216, Ser214, Leu212, Pro261, Thr19, Trp111, Tyr48, Gln183, Lys77, and Ile260 formed van der Waals interactions with apigenin, the best binding ligand.

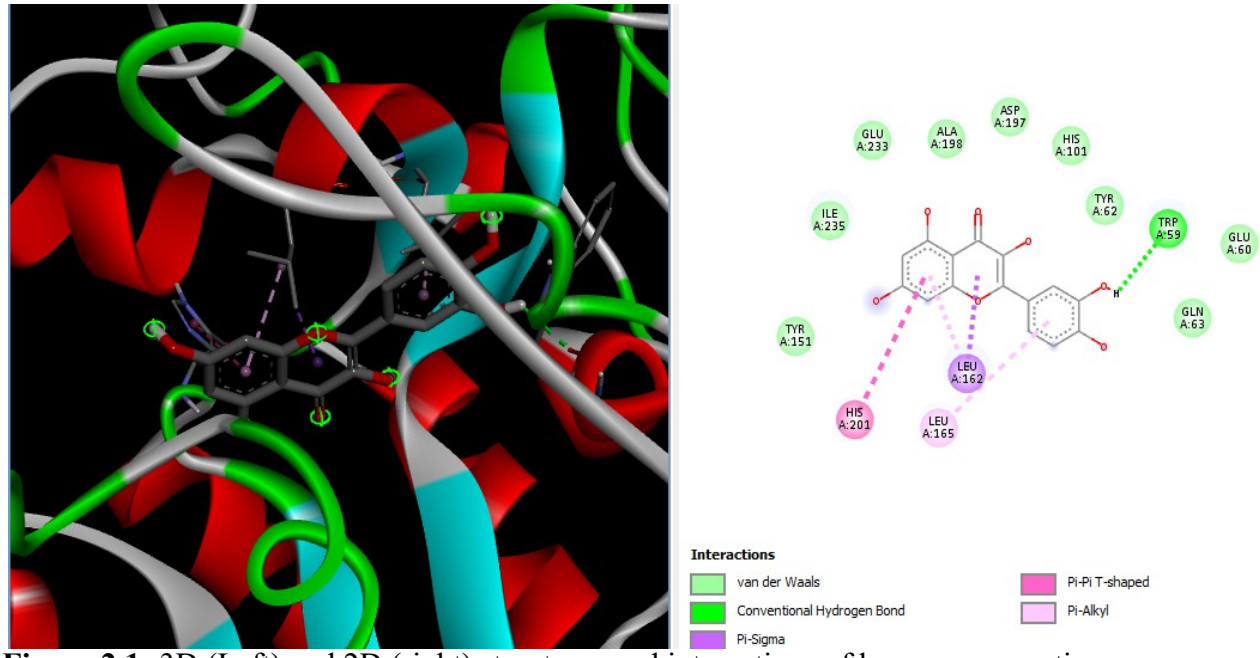

Figure 2.1: 3D (Left) and 2D (right) structures and interactions of human pancreatic α-amylase docked with quercetin

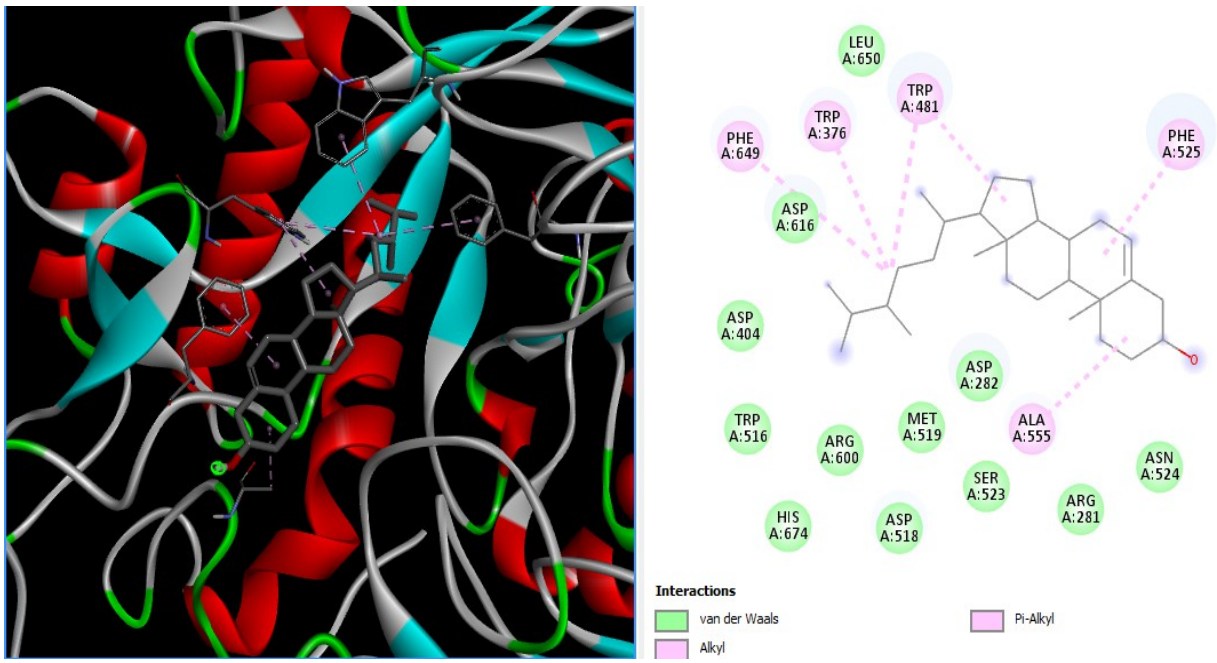

Figure 2.2: 3D (left) and 2D (right) structures and interactions of human α-glucosidase docked with campesterol.

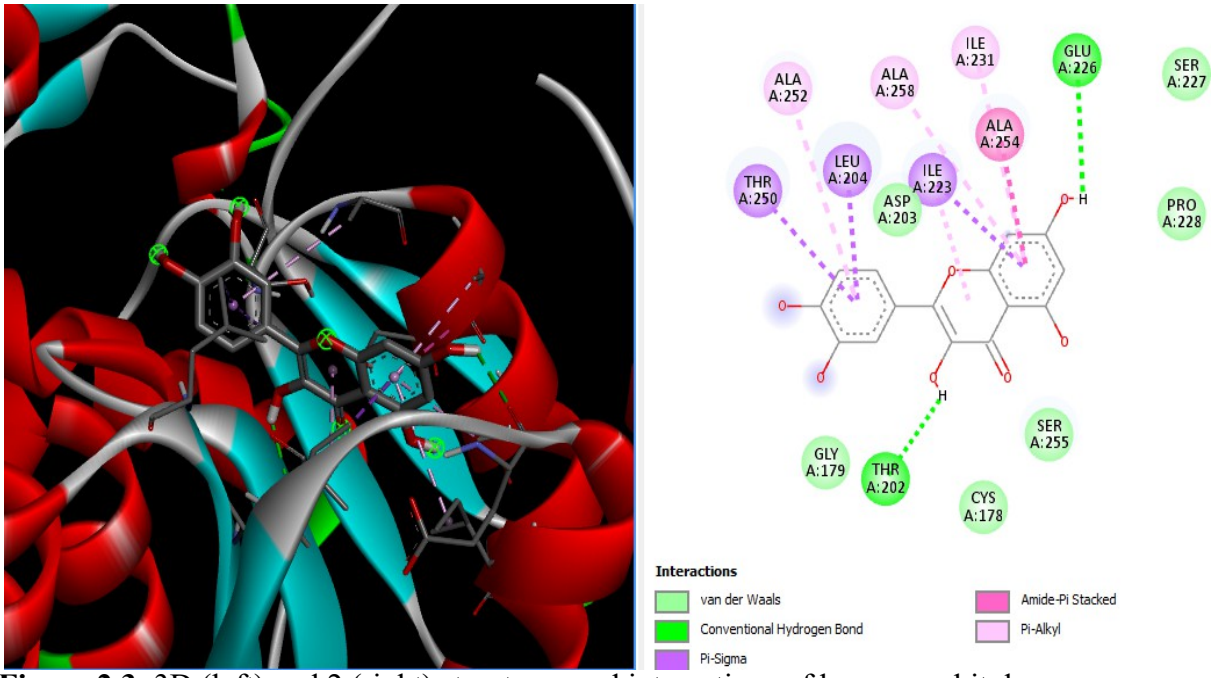

Figure 2.3: 3D (left) and 2 (right) structures and interactions of human sorbitol dehydrogenase docked with quercetin.

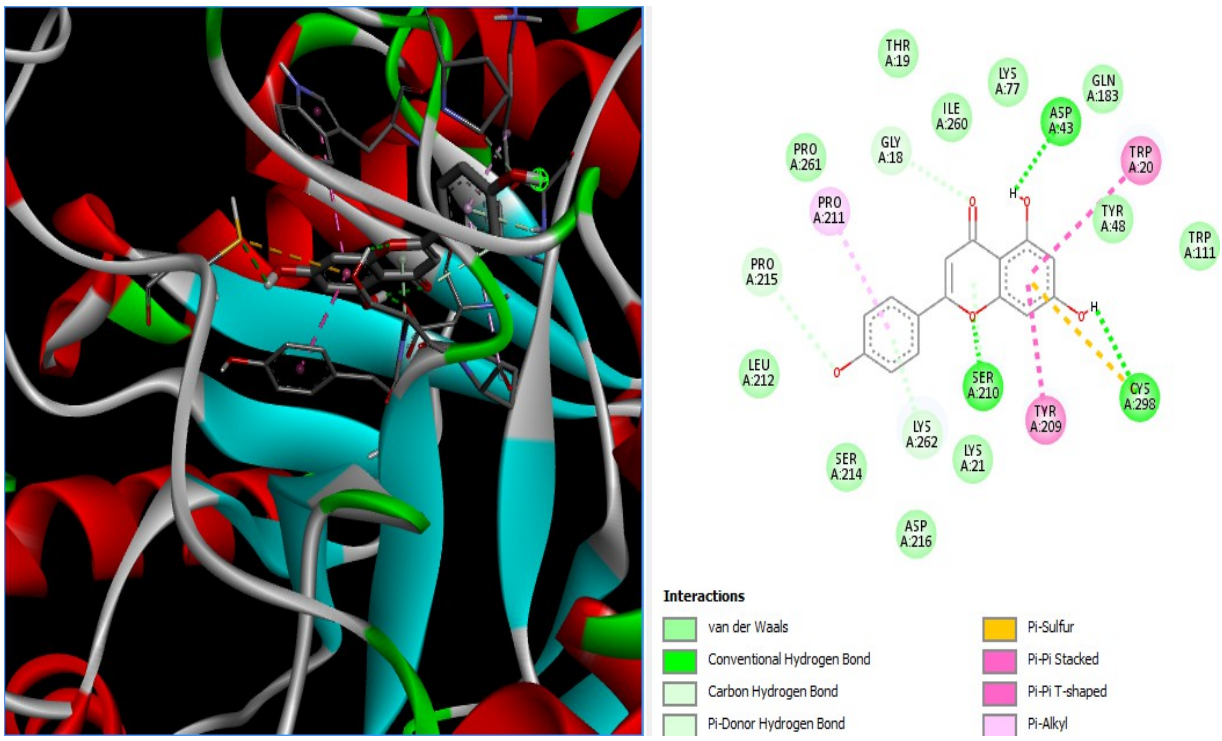

Figure 2.4: 3D (left) and 2D (right) structure and interactions of human aldose reductase docked with apigenin.

The top ten (10) ligands according to their binding affinities (kcal/ mol) are presented in Table 2. The lower the binding energy, the better the binding affinity and ligand. Here, the compound apigenin is revealed as the overall best ligand because of its binding energy of -9.8 kcal/mol.

Table 2: Top ten (10) ligands and their binding affinities with each target protein.

S. No.	Ligands	PubChem ID	Diabetic protein targets α-amylase	α-glucosidase	AR	SDH
1	Apigenin	5280443	-7.5	-7.2	**-9.8**	-7.4
2	Luteolin	5280445	-7.4	-7.0	-9.7	-8.4
3	Kaempferol	5280863	-7.6	-7.0	-9.5	-6.7
4	Quercetin	5280343	**-7.8**	-6.8	-9.5	**-8.5**
5	Capsaicin	1548943	-6.0	-6.3	-9.1	-5.8
6	Campesterol	173183	-7.1	**-8.3**	-5.3	-7.8
7	Stigmasterol	5280794	-7.2	-8.2	-7.4	-8.1
8	Caffeic acid	689043	-6.5	-6.0	-8.2	-6.2
9	26-Hydrocholesterol	99470	-6.5	-8.1	-7.6	-7.0
10	Beta-Sistosterol	22284	-6.8	-8.1	-5.0	-6.9
11	Tolrestat*	53359	-	-	-6.5	-7.3
12	Acarbose*	41774	-4.7	-7.2	-	-

* Denotes standard drugs used in this study.

The physicochemical properties of the best ten (10) ligands embedded in *Musa paradisiaca* aqueous pulp extract are presented in Table 3.1. From the table, the compounds embedded in the plant obeyed the Lipinski rule of five (RO5) which states that a molecule is more likely to be druggable if it has no more than five violations of the following criteria: molecular weight less than 500, logP less than 5, hydrogen bond donors less than 5, hydrogen bond acceptors less than 10, and 10 or fewer rotatable bonds.

The assessment of water solubility and lipophilicity properties of the top ten (10) ligands is presented in Table 3.2. Stigmasterol showed the best logarithm of the partition coefficient (log P) with a value of 5.08. Apigenin, luteolin, quercetin, kaempferol, capsaicin, and caffeic acid are the only ligands predicted to be water-soluble. Meanwhile, all other ligands are also within the ranges away from zero (0), indicating their good lipophilicity properties.

The top ten (10) ligands have a good bioavailability score of 0.55, which is a good drug-likeness property since a minimum of 0.10 bioavailability score is required of a compound to become a drug candidate. All ten ligands obey Lipinski's rule of five (RO5) and Veber. However, only five (5) compounds obeyed Muegge's rule, and six (6) compounds obeyed Egan's rule (Table 3.3).

The medicinal chemical properties of the overall top ten (10) ligands are presented in Table 3.4. Seven of the top ten ligands showed positive pan-assay interference compounds (PAINS), and four ligands showed positive lead-likeness indications. This indicates that the test compounds are not likely to give false-positive results in high-throughput screenings. All the top ten ligands indicated that the synthetic accessibility scored approximately from 1.81 – 6.30, where beta-sitosterol showed the best synthetic accessibility.

The pharmacokinetic properties (Table 3.5) showed low gastrointestinal absorption for three of the ten best ligands, including campesterol, stigmasterol, and beta-sitosterol. Moreso, the blood-brain barrier permeability showed a positive indication for one of these best ten ligands, whereas no ligand was identified as a P-glycoprotein substrate. Five of the best ten ligands were predicted to be CYP34A4 inhibitors. Meanwhile, no ligand was identified as an inhibitor of CYP2C19. Similarly, apigenin, luteolin, kaempferol, quercetin, and capsaicin were identified as inhibitors of CYP1A2 and CYP2D6. Additionally, stigmasterol is the only ligand identified to

be a CYP2C9 inhibitor.

All the selected ligands have a negative indicator for kidney and carcinogenic toxicity. Two of the ten best ligands, including apigenin and caffeic acid, show a negative indicator for respiratory and mitochondrial toxicity. Additionally, luteolin, capsaicin, and caffeic acid have a negative indicator for hepatotoxicity, while all ten ligands have negative indicators for reproductive toxicity (Table 3.6).

The absorption, distribution, metabolism, excretion, and toxicity (ADME/T) properties of the overall top ten (10) ligands are presented in Tables 3.1-3.6.

Table 3.1: Physicochemical properties of active compounds embedded in *Musa paradisiaca* pulp.

Ligands	Molecular Formula	Molecular Weight (g/mol)	NRB	NHBA	NHBD
Apigenin	$C_{15}H_{10}O_5$	270.24	1	5	3
Luteolin	$C_{15}H_{10}O_6$	286.24	1	6	4
Kaempferol	$C_{15}H_{10}O_6$	286.24	1	6	4
Quercetin	$C_{15}H_{10}O_7$	302.24	1	7	5
Capsaicin	$C_{18}H_{27}NO_3$	305.41	10	3	2
Campesterol	$C_{28}H_{48}O$	400.68	5	1	1
Stigmasterol	$C_{29}H_{48}O$	412.69	5	1	1
Caffeic acid	$C_9H_8O_4$	180.16	2	4	3
26-hydroxy cholesterol	$C_{27}H_{46}O_2$	402.65	6	2	2
Beta-sistosterol	$C_{29}H_{50}O$	414.71	6	1	1
Tolrestat*	$C_{16}H_{14}F_3NO_3S$	357.35	6	6	1
Acarbose*	$C_{25}H_{43}NO_{18}$	645.60	9	19	14

* Denotes standard drugs used in this study. NRB = Number of Rotatable Bonds, NHBA = Number of H-bond Acceptors, NHBD = Number of H-bond Donors

Table 3.2: Water solubility and Lipophilicity properties of *Musa paradisiaca* pulp bioactive compounds

S. No.	Ligands	Log S(ESOL)	Log $P_{o/w}$ (iLOGP)
1	Apigenin	-3.94 (Soluble)	1.89
2	Luteolin	-3.71 (Soluble)	1.86
3	Kaempferol	-3.31 (Soluble)	1.70
4	Quercetin	-3.16 (Soluble)	1.63
5	Capsaicin	-3.53 (Soluble)	3.15
6	Campesterol	-7.54 (Poorly soluble)	4.97
7	Stigmasterol	-7.46 (Poorly soluble)	5.08
8	Caffeic acid	-1.89 (Very soluble)	0.97
9	26-hydroxy	-6.44 (Poorly soluble)	4.60
10	Cholesterol Beta-Sitosterol	-7.90 (Poorly soluble)	5.05
11	Tolrestat*	-4.29 (Moderately soluble)	2.42
12	Acarbose*	2.13 (Highly soluble)	1.43

* Denotes standard drugs used in this study.

Table 3.3: Drug-likeness properties of the bioactive compounds embedded in *Musa paradisiaca* pulp.

S.No	Ligands	Lipinski	Ghose	Veber	Egan	Muegge	Bioavailability score
1	Apigenin	Yes; 0 violation	Yes	Yes	Yes	Yes	0.55
2	Luteolin	Yes; 0 violation	Yes	Yes	Yes	Yes	0.55
3	Kaempferol	Yes; 0 violation	Yes	Yes	Yes	Yes	0.55
4	Quercetin	Yes; 0 violation	Yes	Yes	Yes	Yes	0.55
5	Capsaicin	Yes; 0 violation	Yes	Yes	Yes	Yes	0.55
6	Campesterol	Yes; 1 violation: MLOGP>4.15	No; 2 violations: WLOGP>5.6, #atoms>70	Yes	No; 1 violation: WLOGP>5.88	No; 2 violations: XLOGP3>. Heteroatoms<2	0.55
7	Stigmasterol	Yes; 1 violation: MLOGP>4.15	No; 3 violations: WLOGP>5.6, MR>130, #atoms>70	Yes	No; 1 violation: WLOGP>5.88	No; 2 violations: XLOGP3>. Heteroatoms<2	0.55
8	Caffeic acid	Yes; 0 violation	Yes	Yes	Yes	No; 1 violation: MW<200	0.56
9	26-hydroxy Cholesterol	Yes; 1 violation: MLOGP>4.15	No; 2 violations: WLOGP>5.6, #atoms>70	Yes	No; 1 violation: WLOGP>5.88	No; 1 violation: XLOGP3>5	0.55
10	Beta- Sistoster(	Yes; 1 violation: MLOGP>4.15	No; 3 violations: WLOGP>5.6, MR>130, #atoms>70	Yes	No; 1 violation: WLOGP>5.88	No; 2 violations: XLOGP3>. Heteroatoms<2	0.55
11	Tolrestat*	Yes; 0 violation	Yes	Yes	Yes	Yes	0.56
12	Acarbose*	No; 3 violations: MW>500, NorO>10, NHorOH>5	No; 4 violations: MW>48(WLOGP<- 0.4, MR >130, #atoms>70	No; 1violatior TSAP>140	No; 1 violation: TSAP>131.6	No; 5 violations: MW>600, XLOGP<-2, TPSA>150, H-acc>10, H- don>5	0.17

* Denotes standard drugs used in this study.

Table 3.4: Medicinal chemistry prediction of the bioactive compounds embedded in *M. paradisiaca* pulp extract

S.No	Ligands	PAINS	Brenk	Lead-likeness	Synthetic accessibility
1	Apigenin	0 alert	0 alert	Yes	2.96
2	Luteolin	1alert: catechol_A	1 alert: catechol	Yes	3.02
3	Kaempferol	0 alert	0 alert	Yes	3.14
4	Quercetin	1alert: catechol_A	1 alert: catechol	Yes	3.23
5	Capsaicin	0 alert	1 alert: isolated_ alkene	No;2violations: Rotors>7, XLOGP3>3.5	2.32
6	Campesterol	0 alert	1 alert: isolated_ alkene	No;2violations: MW>350, XLOGP3>3.5	6.17
7	Stigmasterol	0 alert	1 alert: isolated_ alkene	No;2violations: MW>350, XLOGP3>3.5	6.21
8	Caffeic acid	1alert: catechol_A	2 alerts: catech michael_acceptor_1	No;1violation: MW<250	1.81
9	26-hydroxy cholesterol	0 alert	1 alert: isolated_ alkene	No;2violations: MW>350, XLOGP3>3.5	6.09
10	Beta-sistosterol	0 alert	1 alert: isolated_ alkene	No;2violations: MW>350, XLOGP3>3.5	6.30
11	Tolrestat*	0 alert	1 alert: thiocarbonyl_group	No; 2 violations: MW>350, XLOGP3>3.5	2.34
12	Acarbose*	0 alert	1 alert: isolated_ alkene	No; 2 violations: MW>350, Rotors>7	7.34

* Denotes standard drugs used in this study.

Table 3.5: Pharmacokinetics of *Musa paradisiaca* pulp extract bioactive compounds.

S.No	Ligands	GI Absorption	BBB Permeant	P-gp Substrate	CYP1A2 inhibitor	CYP2C19 inhibitor	CYP2C9 inhibitor	CYP2D6 inhibitor	CYP3A4 inhibitor
1	Apigenin	High	No	No	Yes	No	No	Yes	Yes
2	Luteolin	High	No	No	Yes	No	No	Yes	Yes
3	Kaempferol	High	No	No	Yes	No	No	Yes	Yes
4	Quercetin	High	No	No	Yes	No	No	Yes	Yes
5	Capsaicin	High	Yes	No	Yes	No	No	Yes	Yes
6	Campesterol	Low	No	No	No	No	No	No	No
7	Stigmasterol	Low	No	No	No	No	Yes	No	No
8	Caffeic acid	High	No	No	No	No	No	No	No
9	26-hydroxy Cholesterol	High	No	No	No	No	No	No	No
10	Beta-Sistosterol	Low	No	No	No	No	No	No	No
11	Tolrestat*	High	No	No	No	No	Yes	No	No
12	Acarbose*	Low	No	Yes	Yes	Yes	No	No	No

* Denotes standard drugs used in this study.

https://doi.org/10.55549/zbs.1638235

Table 3.6: Toxicity Properties of the bioactive compounds embedded in *Musa paradisiaca* aqueous pulp extract.

S.No	Ligands	Carcinogenic Toxicity	Hepato-toxicity	Respiratory Toxicity	Reproductive Toxicity	Mitochondria Toxicity	Acute Oral toxicity
1	Apigenin	-	+	-	+	-	III
2	Luteolin	-	-	+	+	+	II
3	Kaempferol	-	+	+	+	+	II
4	Quercetin	-	+	+	+	+	II
5	Capsaicin	-	-	+	+	+	III
6	Campesterol	-	+	+	+	+	I
7	Stigmasterol	-	+	+	+	+	I
8	Caffeic acid	-	-	-	+	-	IV
9	26-hydroxy Cholesterol	-	+	+	+	+	III
10	Beta-Sistosterol	-	+	+	+	+	I
11	Tolrestat*	-	+	+	+	+	III
12	Acarbose*	-	+	+	+	+	IV

* Denotes standard drugs used in this study. Toxicity category I is highly toxic and severely irritating, Toxicity category II is moderately toxic and moderately irritating, Toxicity category III is slightly toxic and slightly irritating, and Toxicity category IV is practically non-toxic and not an irritant.

The effect of MPAPE on protein concentrations and glucose levels is presented in Table 4. The administration of MPAPE significantly ($p<0.05$) increased and decreased high levels of glucose and protein concentrations, respectively, compared to the STZ untreated group.

Table 4: Effect of MPAPE on Protein concentrations and Glucose levels

Experimental Groups	Protein Conc. [mg/mL]	Glucose Levels [mg/dL]
Control	0.214 ± 0.06^{a}	82.65 ± 5.82^{a}
STZ	0.131 ± 0.03^{b}	287.80 ± 4.49^{b}
STZ + MPAPE	0.256 ± 0.02^{a}	$114.8\ 0 \pm 3.10^{c}$
STZ + Glb	0.185 ± 0.06^{b}	71.74 ± 1.15^{a}

Data are presented as mean ± SEM (n=6), and values with different alphabets in the same column are statistically significant at $p<0.05$. STZ = Streptozotocin, MPAPE = *Musa paradisiaca* aqueous pulp extract, Glb = Glibenclamide.

The effect of MPAPE on lipid profiles is presented in Table 5. The administration of MPAPE significantly ($p<0.05$) increased the high-density lipoprotein cholesterol (HDL-Chol) compared

to the STZ untreated group. Conversely, MPAPE significantly ($p<0.05$) decreased total cholesterol (total-Chol), triglyceride (TRIG), low-density lipoprotein cholesterol (LDL-Chol), and very low-density lipoprotein cholesterol (VLDL-Chol) compared to the STZ untreated group

Table 5: Effect of MPAPE on Lipid profiles

Experimental Groups	Total-Chol [mg/dL]	TRIG [mg/dL)]	HDL-Chol [mg/dL]	LDL-Chol [mg/dL]	VLDL-Chol [mg/dL]
Control	202.6 ± 1.13^{a}	196.2 ± 2.79^{a}	211.4 ± 9.92^{a}	41.74 ± 0.32^{a}	39.24 ± 0.56^{a}
STZ	599.2 ± 0.38^{b}	452.6 ± 39.18^{b}	102.0 ± 0.99^{b}	148.20 ± 11.28^{b}	148.5 ± 9.84^{b}
STZ + MPAPE	250.0 ± 24.40^{a}	189.2 ± 4.28^{a}	163.7 ± 0.59^{c}	78.47 ± 24.67^{a}	37.83 ± 0.86^{a}
STZ + Glb	295.2 ± 5.76^{a}	237.8 ± 14.07^{a}	184.1 ± 5.73^{c}	55.58 ± 2.64^{a}	50.63 ± 2.27^{a}

Data are presented as mean ± SEM (n=6) with different alphabets in the same column are statistically significant at $p<0.05$. STZ=Streptozotocin, MPAPE=*Musa paradisiaca* aqueous pulp extract, Glb=Glibenclamide.

The effect of MPAPE on antioxidant activities is presented in Figure 3. The administration of MPAPE significantly ($p<0.05$) increased both superoxide dismutase and catalase activities compared to the untreated group. The effect of MPAPE on liver enzyme activities is presented in Figure 4. The administration of MPAPE significantly ($p<0.05$) increased both alanine transferase (ALT) and aspartate transferase (AST) activities compared to the STZ-untreated group.

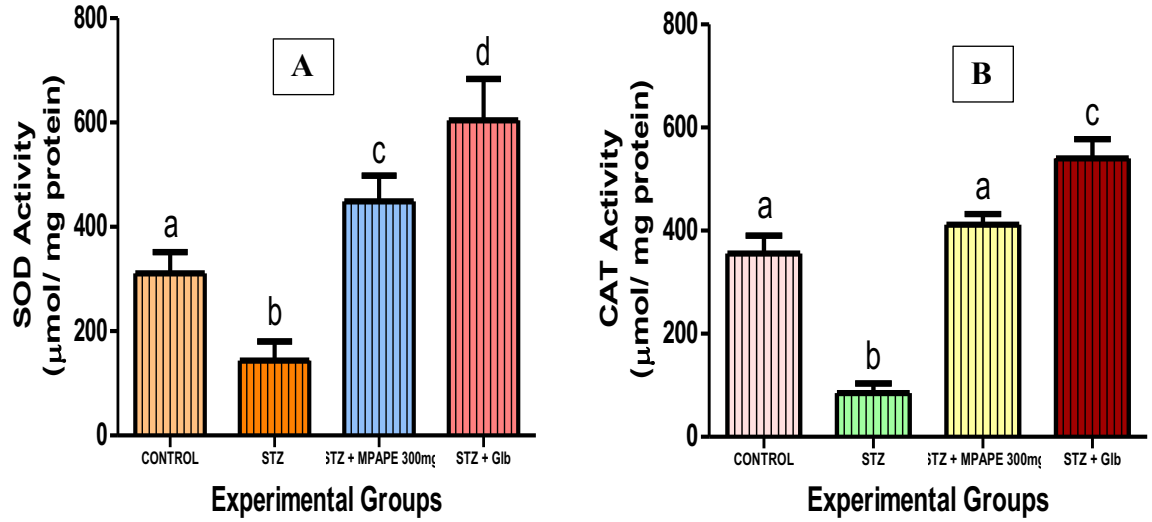

Figure 3: Effects of *Musa paradisiaca* aqueous pulp extract (MPAPE) on antioxidant enzyme: (a) superoxide dismutase and (b) catalase activities in STZ-induced diabetic Wistar rats. Each bar represents mean ± SEM (n=6) and bars with different alphabets are statistically significant at $p<0.05$. STZ=Streptozotocin, Glb=Glibenclamide

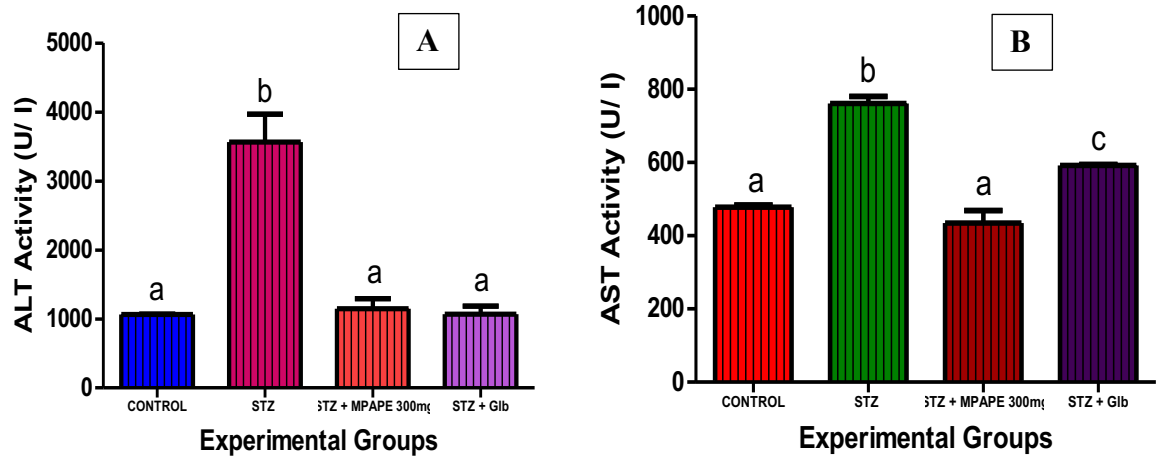

Figure 4: Effects of *Musa paradisiaca* aqueous pulp extract (MPAPE) on liver enzymes: (a) alanine transaminase (ALT) and (b) aspartate transaminase (AST) activities in STZ-induced diabetic Wistar rats. Each bar represents mean ± SEM (n=6), and bars with different alphabets are statistically significant at $p<0.05$. STZ=Streptozotocin, Glb= Glibenclamide

The effects of MPAPE on oxidative stress markers are presented in Table 6. The administration of MPAPE significantly ($p<0.05$) increased glutathione (GSH) compared to the STZ-induced untreated group. Conversely, MPAPE significantly ($p<0.05$) decreased the high hydrogen peroxide (H_2O_2), nitric oxide (NO), and malonaldehyde (MDA) concentration compared to the STZ-induced untreated group.

Table 6: Effects of MPAPE on oxidative stress markers

Experimental Groups	H_2O_2 [mmol/mL]	NO [mmol/mL]	GSH [µmol/mg protein]	MDA [nMoles]
Control	0.053 ± 0.01^a	0.038 ± 0.01^a	339.80 ± 13.78^a	80.02 ± 2.75^a
STZ	0.190 ± 0.04^b	0.156 ± 0.01^b	191.60 ± 7.020^b	197.40 ± 0.87^b
STZ + MPAPE	0.045 ± 0.00^a	0.054 ± 0.01^a	410.30 ± 61.88^c	68.05 ± 0.03^a
STZ + Glb	0.060 ± 0.00^a	0.037 ± 0.00^a	392.50 ± 6.83^a	58.61 ± 2.12^a

Data are presented as mean ± SEM (n=6), and values with different alphabets in the same column are statistically significant at $p<0.05$. STZ=Streptozotocin, MPAPE=*Musa paradisiaca* aqueous pulp extract, Glb=Glibenclamide, MDA=malonaldehyde, GSH=glutathione, NO=nitric oxide, H2O2=hydrogen peroxide.

Discussion

Individuals diagnosed with diabetes mellitus are more likely to develop complications due to hyperglycemia. The use of conventional drugs in the management of diabetes has been associated with adverse effects that are detrimental to the health of individuals, which has given

grounds for the exploration of medicinal plants as an alternative treatment (Idm'hand *et al*., 2020). The phytochemical screening of *M. paradisiaca* aqueous pulp extract confirmed the presence of flavonoids, alkaloids, phenols, tannins, and saponins, but not terpenoids and steroids. These phytochemicals (bioactive compounds) act as antioxidants by exerting their protective effects on the cells of the body and acting as immune regulators, scavengers of reactive oxygen species (ROS), and preventers of ROS generation (Vo *et al*., 2020).

If scientifically proven, the phytochemicals embedded within a medicinal plant that contain biochemical properties with known pharmacological activities are used to develop modern medicine for the treatment and management of various illnesses, including diabetes and its complications (Awuchi, 2019). Alkaloids are a group of nitrogen-containing compounds, obtained from plants that possess pharmacological properties, such as analgesic, anticancer, antibacterial, antimalarial, and antidepressant activities (Adibah and Azzreena, 2019). Flavonoids and phenols are secondary metabolites that also serve as antioxidants that scavenge and eliminate free radicals. They have also shown effective antioxidant, anticancer, antibacterial, and anti-inflammatory properties while improving the immune system (Tungmunnithum *et al*., 2018). The quantitative analysis of the aqueous fruit pulp extract of *Musa paradisiaca* showed a high polyphenolic content of total flavonoids, followed by total phenols and total tannins.

Molecular docking is an essential computational technique in developing new drugs for various disease management and treatment. It forecasts the interactions between a possible medication and its target protein and aids in assessing the feasibility of therapeutic candidates (Riyaphan *et al*., 2021). In this study, to determine the antidiabetic potential and prospects of the phytochemical constituents of *M. paradisiaca* aqueous fruit pulp extracts (MPAPE), an extensive *in silico* approach was employed. The compounds obtained from GC-MS and HPLC analysis of the extract served as the ligands alongside the standard drugs tolrestat and acarbose. All were selected and docked against the catalytic sites of four different diabetic target proteins, and the docking scores were obtained. Figures 2.1 – 2.4 show the interacting amino acids and bonds responsible for the stability of the protein-ligand complex. The active site of each of the proteins contains different amino acid residues, such that α-amylase contains His201, Leu162, Trp59, and Leu165. As well as, Try151, Ile235, Glu233, Ala198, Asp197, His101, Glu60, Tyr62, and Gln63. Some of the amino acid residues present at the active sites of other protein such as α-glucosidase includes Leu650, Asp616, Asn524, Asp404, Asp282, Arg281, Ser253, Met519, Asp518, Arg600, His647, and Trp516; sorbitol dehydrogenase includes Thr250, Leu204, Ile233, Ala252, Ser255, Cys178, Gly179, Glu226, and Pro228, and aldose reductase includes Lys21, Asp216, Ser214, Leu212, Pro261, Thr19, Trp111, Tyr48, Gln183, Lys77, and Ile260. The results showed campsterol, apigenin, and quercetin as the top binding ligands of each protein target.

In the last decade, drug failures due to poor pharmacokinetic profiles, medicinal chemistry properties, efficacy, unmanaged toxicity, and inadequate drug-likeness properties have been on the rise. This led to a focus on improving the drug development process by utilizing ADMET properties at the early stages (Dulsat *et al*., 2023). In this study, the ADMET properties of the top ten (10) ligands resulting from the *in-silico* study were analyzed using SwissADME, admetSAR, and ProTox software. All the best ten (10) ligands obeyed the Lipinski rule of five (RO5) (Lipinski, 2004), which shows that all ten ligands have the potential to be used in the development of new pharmaceuticals (Ivanović *et al*., 2020). Stigmasterol showed the best logarithm of the partition coefficient (log P) with a value of 5.08. Apigenin, luteolin, quercetin, kaempferol, capsaicin, and caffeic acid are the only ligands predicted to be water-soluble. Meanwhile, the remaining ligands, campesterol, stigmasterol, 26-hydro cholesterol, and beta-

sitosterol are within the ranges away from zero (0), indicating their good lipophilicity properties. This aligns with similar studies by Chmiel *et al*. (2019). Drug-likeness properties showed that all ten ligands have a good bioavailability score range of 0.17 to 0.55, since a minimum of 0.10 bioavailability score is required for a compound to become a drug candidate (Ntie-Kang *et al*., 2019).

The medicinal chemistry prediction of the top ten ligands showed that seven of these ligands have positive pan-assay interference compounds (PAINS), and four ligands showed positive lead- likeness indications. This indication may imply that these compounds are not likely to give false-positive results in high-throughput screenings. More so, all the top ten ligands indicated a synthetic accessibility score range of 1.81 to 6.30, where beta-sitosterol showed the best synthetic accessibility. This may imply that this compound can be easily used in the synthesis of a new drug (Stratton *et al*., 2015). Pharmacokinetic properties of the overall top ten ligands showed low gastrointestinal absorption for three of the ten best ligands, including campesterol, stigmasterol, and beta-sitosterol. Additionally, the blood-brain barrier permeability showed a positive indication for one of the ligands, as a result, this compound may be developed and used for central nervous system (CNS) disorders, especially in neurological disorders, including dementia, schizophrenia, and Alzheimer's disease (Małkiewicz *et al*., 2019). Whereas no ligand was identified as a P-glycoprotein substrate. Five of the best ten ligands were predicted to be CYP34A4 (cytochrome P450 3A4) inhibitors. Meanwhile, no ligand was identified as an inhibitor of CYP2C19 (cytochrome P450 2C19). Similarly, apigenin, luteolin, kaempferol, quercetin, and capsaicin were identified as inhibitors of CYP1A2 (cytochrome P450 1A2) and CYP2D6 (cytochrome P450 2D6C). Additionally, stigmasterol is the only ligand identified to be a CYP2C9 (cytochrome P450 2C9) inhibitor.

Streptozotocin (STZ) is a chemical agent used experimentally in the partial or total destruction of pancreatic islet β-cells in animal models to induce either type 1 diabetes mellitus (T1DM) or type 2 diabetes mellitus (T2DM) (Furman, 2015). In this present study, the STZ-induced diabetic Wistar rats exhibited the characteristic hyperglycemia attributed to diabetes mellitus. The induced hyperglycemia was, however, reduced after the oral administration of MPAPE (300 mg/ kg body weight) over 21 days. This suggests that MPAPE has a hypoglycemia potential by increasing the glucose uptake (Taylor *et al*., 2021). On the other hand, STZ intraperitoneal injection also caused a significant ($p<0.05$) decrease in the protein concentration of the STZ-untreated animals compared to the control. However, the oral administration of 300 mg/kg bw of MPAPE and glibenclamide significantly ($p<0.05$) decreased the concentration in the STZ-induced rats.

Initially, the induction of diabetes using STZ resulted in a significant increase in glucose (hyperglycemia), lipids (hyperlipidemia), and alterations in liver enzymes. However, following the administration of MPAPE (300 mg/ kg body weight), a significant decrease ($p<0.05$) was observed in these parameters. This aligns with the findings of Salazar-García and Corona, (2021) who reported similar findings after treatment Superoxide dismutase (SOD) and catalase (CAT) are enzymatic antioxidants that are crucial in the mitigation of free radical-induced oxidative stress (Kumar and Pandey, 2015). SOD facilitates the dismutation of super-oxides produced during enzymatic and non-enzymatic processes in the biological system (Fujii *et al*., 2022). On the other hand, CAT neutralizes the H_2O_2 produced during the dismutation process to prevent oxidative stress and protect the cells (Tehrani and Moosavi-Movahedi, 2018). The treatment of STZ-induced diabetic rats with MPAPE (300 mg/ kg body weight) restored the plasma antioxidant levels.

Hyperglycemia triggered by STZ-induction may lead to an increase in polyunsaturated (PUFA)

fatty acids in the cell membrane, leading to lipid peroxidation (Manirafasha, 2014). In this study, there was a significant increase in the plasma malonaldehyde (MDA), hydrogen peroxide (H_2O_2), and nitric oxide (NO) levels of the STZ untreated animals compared to the control. However, following the administration of MPAPE (300 mg/ kg body weight) and glibenclamide, there was a significant decrease in these parameters. This improvement in oxidative stress markers is most likely attributed to the embedded phytochemicals of MPAPE and its ability to scavenge and neutralize free radicals.

The liver enzymes, alanine transaminase (ALT) and aspartate transaminase (AST), serve as indicators of hyperglycemia-induced liver damage/injury (Mohamed *et al*., 2016). In this study, the activities of the liver enzymes (ALT and AST) significantly ($p<0.05$) increased in the STZ untreated rats, which is an indicator of liver damage or injury. However, treatment with MPAPE (300mg/ kg body weight) and the standard drug, glibenclamide, significantly ($p<0.05$) decreased the activities of the plasma liver enzyme of the STZ untreated animals. Similar findings have been reported by McGill (2016).

Conclusion

In conclusion, the evaluation of *Musa paradisiaca* fruit aqueous pulp extract provided evidence to the traditional claim that the plant contains bioactive compounds that show significant antidiabetic potential. This embedded bioactive compound possesses insulin-releasing properties as indicated by the reduction of glucose levels, in addition to its ability to mitigate oxidative stress induced by reactive oxygen species (ROS) via STZ introduction to a biological system (Wistar rat).

Declaration of Conflict of Interest

The authors of this research declare no known financial or any other conflict of interest.

Authors and Contribution

O.K.A. developed the concept, designed experiments, reviewed, and edited the manuscript.

A.A.A. carried out the investigation and wrote the first draft.

References

Adeniran, A., Anjorin, O. & Chieme, C. (2022). Prevalence and Risk Factor of Diabetes Mellitus among Civil Servants in Abeokuta Town, Ogun State, Nigeria. *Tropical Journal of Medical Research,* 21**,** 29-37.

Adetuyi, B. O., Odine, G. O., Olajide, P. A., Adetuyi, O. A., Atanda, O. O. & Oloke, J. K. (2022). Nutraceuticals: role in metabolic disease, prevention and treatment. *World News of Natural Sciences,* 42**,** 1-27.

Adibah, K. Z. M., & Azzreena, M. A. (2019). Plant toxins: alkaloids and their toxicities. *GSC Biological and Pharmaceutical Sciences*, *6*(2), 21-29.

Awote, O. K., Amisu, K. O., Anagun, O.S., Dohou, F. P., Olokunola, E. R., & Elum, N. O. (2024). *In vitro* and Molecular Docking Evaluation of the Antibacterial, Antioxidant, and Antidiabetic Effects of Silver Nanoparticles from *Cymbopogon citratus* Leaf. *Tropical Journal of Natural Product Research (TJNPR)*, *8*(9): 8400–8411.

Awote, O. K., Adeyemo, A. G., Igbalaye, J. O., Awosemo, R. B., Ibrahim, A. B., Omolaja, B. E., Abdulrafiu, F., & Fajobi, T. (2021a). *In vitro* alpha-amylase inhibitory activity, antioxidant activity and HPLC analysis of Eichhornia crassipes (water hyacinth) methanol extracts.

Awote, O. K., Igbalaye, J. O., & Adeyemo, A. G. (2021b). Effect of *Phragmanthera incana* Leaves Extracts on Lipid Profile in Wistar Rats Fed High-Fat Diet. *International Journal of Formal Sciences: Current and Future Research Trends*, *12*(1), 23-32.

Awuchi, C. G. (2019). Medicinal plants: the medical, food, and nutritional biochemistry and uses. *International Journal of Advanced Academic Research*, *5*(11), 220-241.

Ayeni, E. A., Gong, Y., Yuan, H., Hu, Y., Bai, X. & Liao, X. (2022). Medicinal plants for anti-neurodegenerative diseases in West Africa. *Journal of Ethnopharmacology,* 285**,** 114468.

Azzi, A. (2022). Oxidative stress: what is it? Can it be measured? Where is it located? Can it be good or bad? Can it be prevented? Can it be cured? *Antioxidants,* 11**,** 1431.

Banu, S., & Bhowmick, A. (2017). Therapeutic targets of type 2 diabetes: An overview. *MOJ Drug Des. Dev. Ther*, *1*(11).

Chmiel, T., Mieszkowska, A., Kempińska-Kupczyk, D., Kot-Wasik, A., Namieśnik, J., & Mazerska, Z. (2019). The impact of lipophilicity on environmental processes, drug delivery and bioavailability of food components. *Microchemical Journal*, *146*, 393-406.

Daliri, E. B. M., Oh, D. H., & Lee, B. H. (2017). Bioactive peptides. *Foods*, *6*(5), 32.

Dulsat, J., López-Nieto, B., Estrada-Tejedor, R., & Borrell, J. I. (2023). Evaluation of free online ADMET tools for academic or small biotech environments. *Molecules*, *28*(2), 776.

Fagbohun, O. F., Oriyomi, O. V., Adekola, M. B., & Msagati, T. A. Biochemical applications of *Kigelia africana* (Lam.) Benth. fruit extracts in diabetes mellitus. *Comparative Clinical Pathology*, 2020, 29, 1251-64.

Fasula, J., Adejumo, B., Akhaumere, E., Oke, M., Odionyenma, U., Dimkpa, U. & Abdulkadir, U. 2024. Prevalence and Risk Factors Associated with Diabetes mellitus among children of parents living with Diabetes in Ondo State, Nigeria. *Open Journal of Medical Research (ISSN: 2734-2093),* 5**,** 1-15.

Fujii, J., Homma, T., & Osaki, T. (2022). Superoxide radicals in the execution of cell death. *Antioxidants*, *11*(3), 501.

Furman, B. L. (2015). Streptozotocin-induced diabetic models in mice and rats. *Current protocols in pharmacology*, *70*(1), 5-47.

Ghasemi, A., & Jeddi, S. (2023). Streptozotocin as a tool for induction of rat models of diabetes: A practical guide. *EXCLI journal*, *22*, 274.

Google Search Engine (2025).

Green, L. C., Wagner, D. A., Glogowski, J., Skipper, P. L., Wishnok, J. S., & Tannenbaum, S. R. (1982). Analysis of nitrate, nitrite, and [15N] nitrate in biological fluids. *Analytical biochemistry*, *126*(1), 131-138.

Idm'hand, E., Msanda, F., & Cherifi, K. (2020). Ethnopharmacological review of medicinal plants used to manage diabetes in Morocco. *Clinical Phytoscience*, *6*, 1-32.

Ivanović, V., Rančić, M., Arsić, B., & Pavlović, A. (2020). Lipinski's rule of five, famous extensions and famous exceptions. *Popular Scientific Article*, *3*(1), 171-177.

Jollow, D. J., Mitchell, J. R., Zampaglione, N. A., & Gillette, J. R. (1974). Bromobenzene-induced liver necrosis. Protective role of glutathione and evidence for 3, 4-bromobenzene oxide as the hepatotoxic metabolite. Pharmacology, 11(3): 151-169.

Kemisetti, D., & Rajeswar Das, D. B. B. (2022). A comprehensive review on *Musa paradisiaca* taxonomical, morphological classification and its pharmacological activities. *Journal of Pharmaceutical Negative Results*, 737-749.

Kumar, S., & Pandey, A. (2015). Free radicals: health implications and their mitigation by herbals. *British Journal of Medicine and Medical Research*, *7*(6), 438-457.

Lipinski, CA. (2004). Lead-and drug-like compounds: the rule-of-five revolution. *Drug Discovery Today: Technologies,* 1(4): 337-41.

Lowry, O.H., Rosebrough, N.J., Farr, A.L., Randall, R.J., 1951. Protein measurement with the Folin phenol reagent. Journal of Biological Chemistry, 193: 265–275.

Małkiewicz, M. A., Szarmach, A., Sabisz, A., Cubała, W. J., Szurowska, E., & Winklewski, P. J. (2019). Blood-brain barrier permeability and physical exercise. *Journal of neuroinflammation*, *16*, 1-16.

Manirafasha, C. (2014). *The effects of kolaviron on epididymal and testicular function in streptozotocin induced diabetic wistar rats* (Doctoral dissertation, Cape Peninsula University of Technology).

Marino, A., Battaglini, M., Moles, N., & Ciofani, G. (2022). Natural antioxidant compounds as potential pharmaceutical tools against neurodegenerative diseases. *ACS omega*, *7*(30), 25974-25990.

McGill, M. R. (2016). The past and present of serum aminotransferases and the future of liver injury biomarkers. *EXCLI journal*, *15*, 817.

Mohamed, J., Nafizah, A. N., Zariyantey, A. H., & Budin, S. (2016). Mechanisms of diabetes-induced liver damage: the role of oxidative stress and inflammation. *Sultan qaboos university medical journal*, *16*(2), e132.

Ntie-Kang, F., Nyongbela, K. D., Ayimele, G. A., & Shekfeh, S. (2019). "Drug-likeness" properties of natural compounds. *Physical Sciences Reviews*, *4*(11), 20180169.

Ogunyinka, B.I., Oyinloye, B.E., Osunsanmi, F.O., Opoku, A.R., & Kappo, A.P. (2017). Protective effects of *Parkia biglobosa* protein isolate on streptozotocin-induced hepatic damage and oxidative stress in diabetic male rats. Molecules, 22(10): 1654.

Oladimeji, S.O., Soares, A.S., Igbalaye, J.O., Awote, O.K., Adigun, A.K., & Awoyemi, Z.O. (2022). Ethanolic Root Extract of *Urtica dioica* Exhibits Pro-fertility and Antioxidant Activities in Female Albino Rats. *International Journal of Biochemistry Research & Review*. 31(8):29-38.

Oladimeji, S.O., Igbalaye, J.O., Awote, O.K., Shodimu, B.O., Oladeinde, D.T., Omorowa, V.T., Oluwole, S.M., Akinyemi, Y.A., Shobowale, A.Y., Jimoh, D., & Balogun, S.T. (2023). *Cissampelos pareira* ethanolic extract modulates hormonal indices, lipid profile, and oxidative parameters in transient infertility-induced female albino rats. *Bio-Research*, *21*(2), pp.1961-1972.

Onah, L. U., & Oguche, S. O. (2022). Histopathological Analysis of the Kidney of Alloxan Induced Diabetic Albino (Wistar Strain) Rat Treated with Musa paradisiaca (Plantain) Stem Juice. *Int. J. Sci. Res. in Chemical Sciences, 9*(2): 8-13.

Ortiz, G. G., Huerta, M., González-Usigli, H. A., Torres-Sánchez, E. D., Delgado-Lara, D. L., Pacheco-Moisés, F. P., Mireles-Ramírez, M. A., Torres-Mendoza, B. M., Moreno-Cih, R. I., & Velázquez-Brizuela, I. E. (2022). Cognitive disorder and dementia in type 2 diabetes mellitus. *World Journal of Diabetes*, *13*(4), 319.

Padhi, S., Nayak, A. K., & Behera, A. (2020). Type II diabetes mellitus: a review on recent drug- based therapeutics. *Biomedicine & Pharmacotherapy*, *131*, 110708.

Riyaphan, J., Pham, D. C., Leong, M. K., & Weng, C. F. (2021). In silico approaches to identify polyphenol compounds as α-glucosidase and α-amylase inhibitors against type-II diabetes. *Biomolecules*, *11*(12), 1877.

Saeedi, P., Petersohn, I., Salpea, P., Malanda, B., Karuranga, S., Unwin, N., Colagiuri, S., Guariguata, L., Motala, A. A., Ogurtsova, K. & Shaw, J. E. (2019). Global and regional diabetes prevalence estimates for 2019 and projections for 2030 and 2045: Results from the International Diabetes Federation Diabetes Atlas. *Diabetes research and clinical practice*, *157,* 107843.

Salazar-García, M., & Corona, J. C. (2021). The use of natural compounds as a strategy to counteract oxidative stress in animal models of diabetes mellitus. *International Journal of Molecular Sciences*, *22*(13), 7009.

Shree, R. L., & Selvakumar, P. (2022) Phytochemical and Pharmacological Property Review of

Musa Paradisiaca. *YMER, 21(11): 152-166.*

Singh, A., Kukreti, R., Saso, L., & Kukreti, S. (2022). Mechanistic insight into oxidative stress-triggered signaling pathways and type 2 diabetes. *Molecules*, *27*(3), 950.

Stratton, C. F., Newman, D. J., & Tan, D. S. (2015). Cheminformatic comparison of approved drugs from natural product versus synthetic origins. *Bioorganic & medicinal chemistry letters*, *25*(21), 4802-4807.

Taylor, S. I., Yazdi, Z. S., & Beitelshees, A. L. (2021). Pharmacological treatment of hyperglycemia in type 2 diabetes. *The Journal of clinical investigation*, *131*(2), e142243.

Tehrani, H. S., & Moosavi-Movahedi, A. A. (2018). Catalase and its mysteries. *Progress in biophysics and molecular biology*, *140*, 5-12.

Tungmunnithum, D., Thongboonyou, A., Pholboon, A., & Yangsabai, A. (2018). Flavonoids and other phenolic compounds from medicinal plants for pharmaceutical and medical aspects: An overview. *Medicines*, *5*(3), 93.

Varshney, R., & Kale, R. K. (1990). Effects of calmodulin antagonists on radiation-induced lipid peroxidation in microsomes. *International journal of radiation biology*, *58*(5), 733-743.

Wolff, S. P. (1994). Ferrous ion oxidation in the presence of ferric ion indicator xylenol orange for measurement of hydroperoxides. Methods in Enzymology, 233: 182–189.

World Health Organization. (2019). *Global action plan on physical Activity 2018-2030: More Active People for a healthier world*. World Health Organization.

Vo, T. T. T., Chu, P. M., Tuan, V. P., Te, J. S. L., & Lee, I. T. (2020). The promising role of antioxidant phytochemicals in the prevention and treatment of periodontal disease via the inhibition of oxidative stress pathways: Updated insights. *Antioxidants*, *9*(12), 1211.

Yedjou, C. G., Grigsby, J., Mbemi, A., Nelson, D., Mildort, B., Latinwo, L., & Tchounwou, P. B. (2023). The management of diabetes mellitus using medicinal plants and vitamins. *International Journal of Molecular Sciences*, *24*(10), 9085.